




# A Framework for Dry Period Low Flow Forecasting in Mediterranean Streams

Konstantina Risva<sup>1</sup> · Dionysios Nikolopoulos<sup>2</sup> · Andreas Efstratiadis<sup>2</sup> · Ioannis Nalbantis<sup>1</sup> 

Received: 6 February 2018 / Accepted: 19 July 2018 /

Published online: 3 September 2018

© Springer Nature B.V. 2018

## Abstract

The objective of this article is to provide a simple and effective tool for low flow forecasting up to six months ahead, with minimal data requirements, i.e. flow observations retrieved at the end of wet period (first half of April, for the Mediterranean region). The core of the methodological framework is the exponential decay function, while the typical split-sample approach for model calibration, which is known to suffer from the dependence on the selection of the calibration data set, is enhanced by introducing the so-called Randomly Selected Multiple Subsets (RSMS) calibration procedure. Moreover, we introduce and employ a modified efficiency metric, since in this modelling context the classical Nash-Sutcliffe efficiency yields unrealistically high performance. The proposed framework is evaluated at 25 Mediterranean rivers of different scales and flow dynamics, including streams with intermittent regime. Initially, signal processing and data smoothing techniques are applied to the raw hydrograph, in order to cut-off high flows that are due to flood events occurring in dry periods, and allow for keeping the decaying form of the baseflow component. We then employ the linear reservoir model to extract the annually varying recession coefficient, and, then, attempt to explain its median value (over a number of years) on the basis of typical hydrological indices and the catchment area. Next, we run the model in forecasting mode, by considering that the recession coefficient of each dry period ahead is a linear function of the observed flow at the end of the wet period. In most of the examined catchments, the model exhibits very satisfactory predictive capacity and is also robust, as indicated by the limited variability of the optimized model parameters across randomly selected calibration sets.

**Keywords** Low flows · Linear reservoir · Recession rate · Savitzky-Golay filter · Randomly selected multiple subsets calibration · Uncertainty

---

✉ Ioannis Nalbantis  
nalbant@central.ntua.gr

Extended author information available on the last page of the article

## 1 Introduction

WMO (1974) defines low flow as the river discharge during *prolonged dry weather*, without clarifying whether this description refers to the systematic decrease of discharge resulting from considerable decrease (or even elimination) of rainfall during the dry period of each hydrological year, or it includes also droughts, which are extreme phenomena that are due to decreased precipitation over longer periods, i.e. annual or multi-annual. In common hydrological practice, low flows refer to a periodic phenomenon, which is an inherent component of the regime of a river. Low flows are associated with the storage dynamics of the catchment, and, particularly, the aquifer outflows. In fact, these are the composite output of several regulation mechanisms through the terrain surface, soil moisture zone and subsoil. In this sense, Hall (1968) defines low flows as “the portion of flow that comes from groundwater or other delayed sources”; thus, low flows depend on multiple factors, including the infiltration characteristics of soils, the extent and hydraulic properties of the aquifers, the rate, frequency and amount of recharge and actual evapotranspiration, as well as the vegetation, topography and climate (Smakhtin 2001; Vafakhah et al. 2014).

In water management practice, the evaluation of low flows is essential for a range of goals, such as water quality management, water supply, irrigation, hydropower planning, environmental flow assessment, and habitat protection. This is also required by the European Water Framework Directive which called for assessing the state of water bodies and establishing environmental constraints for water resources planning and management. To fulfil this requirement, several countries have developed national procedures for low flow assessment, e.g., the UK (Institute of Hydrology 1980; Gustard et al. 1992), Switzerland (Aschwanden and Kan 1999), and Austria (Laaha and Blöschl 2007).

The importance of low flows, from a water management perspective, becomes even more significant in areas characterized by dry climate and excessive water demand, such as many Mediterranean catchments where the water availability reaches its minimum when the water demands are maximal, and vice versa. In particular, across the eastern and southwestern Mediterranean, the dry period, with minimal precipitation, usually lasts from April to October, while the water demands for domestic and agricultural use are major during this period. In those areas, the concurrence of low flows, almost exclusively originating from baseflow, with the increased demands and the absence of major storage works (e.g. reservoirs) may result to substantial water stress. We remark that the aforementioned hydroclimatic characteristics and the associated low-flow problems are not restricted to the Mediterranean region; in fact, the “Mediterranean” climate also embraces the broader California, parts of Western and South Australia, southwestern South Africa, and parts of central coastal Chile (Merheb et al. 2016).

Known approaches for low flow assessment are generally classified into statistical and process-based ones (Laaha et al. 2013). The former mainly aim to estimate low flow characteristics in terms of magnitude, frequency and duration, to be further utilized in water management plans. These characteristics are typically expressed by means of the so-called *low flow indices* representing flow quantiles, durations or deficit volumes, rise/falling rates, etc. In the last three decades, a lot of research has been conducted on regionalization approaches for predicting low flow statistics in ungauged basins (e.g., Vogel and Kroll 1992; Ludwig and Tasker 1993; Smakhtin et al. 1995; Smakhtin 2001; Yu et al. 2002; Kroll et al. 2004; Laaha and Blöschl 2006a; Longobardi and Vallini 2008; Castiglioni et al. 2009; Eslamian et al. 2010; Castiglioni et al. 2011; Tsakiris et al. 2011). Usually, these are based on establishing regression relationships between the low flow characteristics of interest and the

catchment properties (climatic, topographic, meteorological, geological, geomorphological), and, less often, on the usage of hydrological models (e.g., England and Hisdal 2009) or the complementary use of hydrogeological information (e.g., Cervi et al. 2017). In some studies, low flow characteristics are combined with classification approaches that allow for dividing broader areas into homogenous sub-regions, for which different relationships are valid (e.g., Laaha and Blöschl 2006a; Vezza et al. 2010). In few cases, seasonality effects are also accounted for, to distinguish between winter low flows and summer ones, the former being linked to phenomena of snow accumulation and melting (e.g., Schreiber and Demuth 1997; Laaha and Blöschl 2006b; Assani et al. 2011; Farahani and Khalili 2013; Jenicek et al. 2016). Nevertheless, most of the reported regionalization attempts have been made in wet climates, with very few exceptions (e.g., Longobardi and Vallini 2008; Mehaiguene et al. 2012).

It is well-known that a hydrograph can generally be decomposed into rising limbs, reflecting increases in discharge caused by precipitation events, and recession limbs, representing delayed flows due to multiple and complex regulation processes. Process-based approaches aim at representing the recession limb of hydrographs or its individual components, using probabilistic or deterministic simulation models. The exponential decay function is the simplest and most traditional conceptual modelling approach for hydrograph recession analysis (Hall 1968; Singh and Stall 1971; Tallaksen 1995; Gottschalk et al. 1997; Aksoy and Wittenberg 2011). Its first use in hydrology is attributed to Maillet (1905), while its mathematical background originates from Boussinesq (1903), who formulated the idealized problem of outflow from a horizontal, unconfined aquifer discharging into a fully penetrating stream (Brutsaert and Nieber 1977; Eng and Milly 2007). The working hypothesis behind the exponential decay function is the linear reservoir model that represents the recession limb of a hydrograph as the outflow hydrograph from a tank of infinite storage capacity, having no inflows, which implements the groundwater storage. The model is linear since outflow is expressed as a constant fraction of storage, thus resulting in an exponential decay function with a single parameter, i.e. the recession coefficient. In a more general context, a nonlinear relationship between storage and outflow is also considered (typically, of the power-type), which allows better representation of the low-flow regime of complex basins due to the use of two instead of one single parameter (for a comprehensive review of nonlinear recession analysis, please refer to Aksoy and Wittenberg 2011, as well as Akylas et al. 2015). Recently, Fiorotto and Caroni (2013) proposed a stochastic framework to overcome the major shortcoming of the typical hydrograph recession analysis, which ignores the variability in the behavior of individual streamflow recession segments (Tallaksen 1995).

As pointed out by Brandes et al. (2005), process-based methods for estimating recession rates and the associated time scales have not received the same attention as the regionalization ones, despite of their importance in water resources management (for instance, recession scales indicate how rapidly a river reaches dry conditions). Despite of their simplicity, such approaches bear quite large subjectivity in their assumptions (e.g., master recession curves, matching strip, recursive filters, dependence on the starting point with variable initial catchment conditions, etc.), thus resulting in biased and uncertain estimations (Anderson and Burt 1980; Stoelzle et al. 2013).

The prediction, for given starting conditions, of the evolution of future low flow component of a river hydrograph is a typical hydrological forecasting problem. In general, the existing literature approaches refer to short time horizons, which allows for updating the parameters of the forecasting scheme on the basis of new flow data. For instance, Štravs and Brilly (2007) have developed a machine learning method with seven-day lead time for Slovenian rivers, to

be used on a day-to-day operational basis for low flow forecasting during rainless periods. Nicolle et al. (2014) also employed alternative models, already calibrated against observed data in a number of French rivers, considering short (7-day) and medium (30-day) lead times. In a more complex context, Demirel et al. (2013, 2015) took advantage of ensemble meteorological predictions (precipitation, potential evapotranspiration) within conceptual and data-driven models (i.e. artificial neural networks), to provide low flow forecasts for lead times from one up to 90 days; apparently, the success of this approach strongly depends on the uncertainty of seasonal meteorological predictions, which is generally very large.

Nevertheless, in an operational water management context, the time period ahead of a low flow forecasting study may include the entire forthcoming dry period, during which precipitation is expected to be low, or even negligible. Actually, most of the aforementioned forecasting schemes not only are built to represent the recession limb in the short run, but also require systematic flow measurements, thus being applicable only in well-monitored rivers. In this respect, our research objective is to provide a simple yet effective tool for low flow forecasting in the long run (up to six months), with minimal data requirements. In our approach, the low flow component is accounted as the “safe” yield of a river system, i.e. the amount of surface water that can be estimated with quite good accuracy. Simplicity is secured by using as background simulation model the exponential decay function, while data parsimony is ensured by accounting for flow information retrieved at the end of the first half of April, conventionally considered as the end of wet period. This convention is of major importance, since it allows getting timely decisions regarding the optimal allocation of water resources during the entire forthcoming dry period. A stochastic framework, comprising several novelties, has been developed to estimate the regional parameters of the model, on the basis of historical flow data. The proposed framework is tested in 25 Mediterranean rivers from five countries (Spain, France, Italy, Greece and Cyprus), exhibiting very satisfactory predictive capacity and robustness against the inherent uncertainty of the calibration procedure.

## 2 Modelling Framework

### 2.1 Overview and Assumptions

As already explained, our objective is providing a simple forecasting tool to estimate the flow recession during the dry period of each year, by accounting for easily observable hydrological conditions at the end of the antecedent wet period. As the emphasis is on the Mediterranean, for convenience we consider that the dry period has a maximum duration of six months (herein called *reference time horizon*), which extends from April 15th to October 15th; thus the model should be built upon the observed data for the period before April 15th. We emphasize that this convention is made because our approach is oriented to the long-term water management problem; in practice, it is not possible to determine a priori the beginning of the baseflow recession (Rupp and Selker 2006).

In Mediterranean rivers and streams, the low flow component of the dry period hydrograph is mainly attributed to baseflow, which is only slightly influenced by occasional and generally small rainfall events during the dry season. Under such hydroclimatic conditions, a reliable prediction of the temporal evolution of baseflow is essential, since this can be regarded as the guaranteed flow during the dry period. We remind that common low flow forecasting schemes generally consider much shorter lead times, which apparently ensures more accurate

predictions of the recession limbs from multiple (and apparently overlapping) flow regulation sources of both slow (baseflow) and fast (interflow) response.

In order to ensure parsimony and simplicity, we adopt the well-known linear reservoir approach, implying that the catchment (more precisely, the groundwater) storage,  $s(t)$ , is linearly proportional to its outflow,  $q(t)$ , i.e.:

$$s(t) = kq(t) \quad (1)$$

where  $k$  is the so-called recession parameter; in fact, the quantity  $1/k$  represents the mean residence time of the catchment. Under this assumption, for a given discharge at a starting time  $t=0$ , the outflow is expressed by means of an exponential decay function, i.e.:

$$q(t) = q(0)\exp(-kt) \quad (2)$$

In our context, Eq. (2) is expressed in discrete form, considering a daily time interval; thus the model is written as:

$$q_{ij} = q_{0j}\exp(-k_j t_i) \quad (3)$$

where  $q_{ij}$  is the average discharge of day  $i$  and year  $j$ ,  $t_i$  is the accumulated time up to day  $i$ , in day units, and  $q_{0j}$  and  $k_j$  are the annually-varying initial discharge and recession rate, expressed in flow ( $\text{m}^3 \text{s}^{-1}$ ) and inverse time ( $\text{d}^{-1}$ ) units, respectively. For convenience, index  $i=0$  corresponds to the beginning of the dry period, i.e. April 15th, while Eq. (3) is valid up to the end of the dry period, i.e. October 15th, which corresponds to day index  $i=184$ . Therefore, in order to employ (3) in forecasting mode we should simply set  $t_i=i$ .

Given that the Eq. (3) is to be used for forecasting purposes, at the beginning of the dry period (i.e. April 15th) of each year  $j$  it is essential to determine the initial discharge  $q_{0j}$  and the parameter  $k_j$ . Preliminary investigations by Risva et al. (2017) indicated that for the initial discharge, the minimum of the observed daily flow values during the first two weeks of April is the best choice. Therefore, the remaining question involves the “prediction” of the annually-varying recession rate  $k_j$ , based on the available hydrological information up to April 15th. The initial discharge  $q_{0j}$  is considered as predictor, which is evidently associated with the groundwater conditions at the end of the wet period controlling the generation of the dry period baseflow. The simplest dependence relationship is the linear one, thus:

$$k_j = a q_{0j} + b \quad (4)$$

where  $a$  ( $\text{s m}^{-3} \text{d}^{-1}$ ) and  $b$  ( $\text{d}^{-1}$ ) are site-specific parameters that are considered stationary, i.e. not depending on the annually-varying hydrological conditions of the catchment at the end of the wet period. Combining (3) and (4) we obtain the final expression of the forecasting scheme, i.e.:

$$q_{ij} = q_{0j}\exp\left[-\left(a q_{0j} + b\right)t_i\right] \quad (5)$$

The above formula uses a known initial condition at the beginning of each dry period, by means of initial discharge  $q_{0j}$ , and two time-invariant regional parameters,  $a$  and  $b$ . For the estimation of the latter for a specific catchment, we have developed a novel randomly selected multiple subsets calibration framework, wherein Eq. (3) is utilized for recession analysis of observed baseflow data sets across a number of dry periods. The stochastic configuration of the calibration procedure allows for evaluating the uncertainty of the recession model which is

reflected on low flow forecasts; this originates from studies using relatively short historical samples (cf. discussion by Ouarda et al. 2008). Key issues of the proposed framework are:

- The derivation of the baseflow data of each dry period, corresponding to year  $j$  (herein referred to as the *adjusted low flow data*), on the basis of observed daily hydrographs;
- the formulation of a suitable performance measure for evaluating the fitting of the modelled to the observed low flows;
- the implementation of the calibration procedure in a stochastic setting that allows for accounting for the uncertainty of model parameters against the period of observations.

The above issues are discussed in detail in next sections.

## 2.2 Derivation of Adjusted low Flows from Dry Period Data

For a given record of daily flows over the conventional reference period between April 15th and October 15th of a specific year  $j$ , with given starting flow  $q_{0j}$ , the estimation of the recession coefficient  $k_j$  is far beyond a typical calibration problem. In fact, neither the beginning nor the duration of the dry period of each year can be specified a priori, since the dry-period hydrograph contains, apart from the slow response component (which is conventionally attributed to baseflow), both rising and recession limbs, as well as individual peaks that are due to rainfall events.

As shown in the examples given in Fig. 1, attempting to infer  $k_j$  by fitting the exponential decay function (Eq. 3) to the full flow data set spanning over the entire reference period would result in unrealistic and strongly biased (overestimated) values of the recession coefficient. Therefore, before applying the calibration procedure, it is essential to extract the so-called *adjusted low flows* (i.e., values of the baseflow component) for each year  $j$ , and determine the actual start and end of the dry

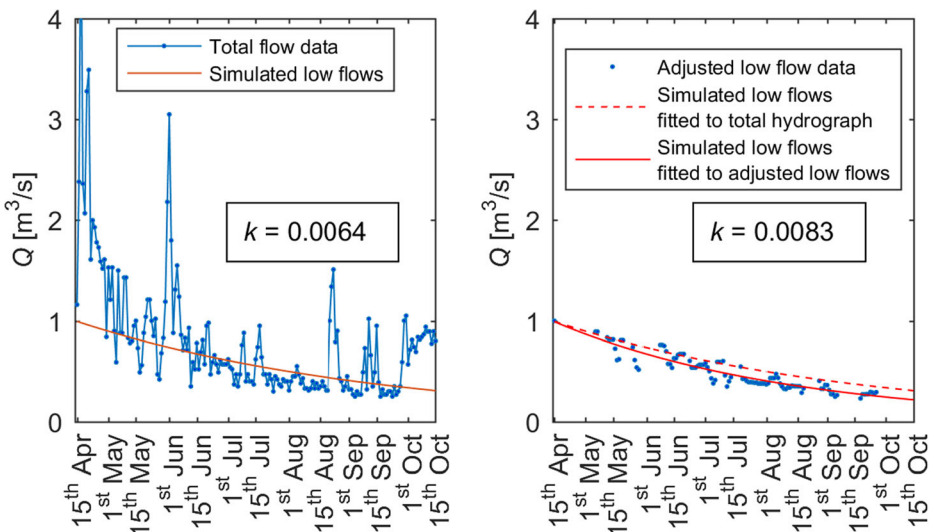


**Fig. 1** Examples of fitting the exponential decay function (3) to the full daily hydrograph over the entire reference period on the left (dotted line on the right), contrasted to the final expression fitted to the adjusted flow data on the right (continuous line). The recession rate is higher when the function is fitted to the adjusted low flows

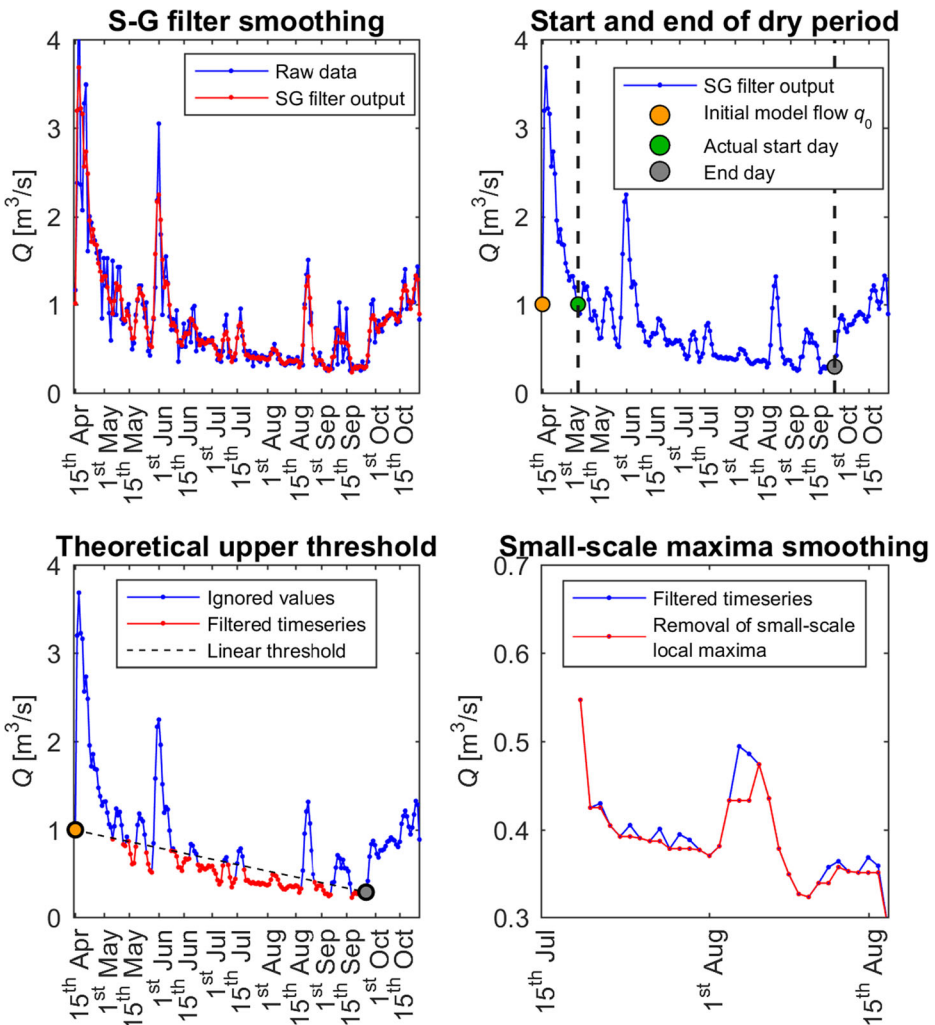


**Fig. 2** Example of extracting the adjusted flow data from the daily hydrograph of Achelous River at Kremasta dam, for the dry period of year 1966

period, the length of which is generally shorter than that of the reference period. In this vein, we employ a multi-step procedure, comprising four steps (see example in Fig. 2):

- Step (a): The full hydrograph over the dry period generally exhibits both large- and small-scale fluctuations; the former are due to flood events, while the latter are often induced by random errors of the monitoring instruments (e.g., stage recorders) or turbidity effects, resulting to local minima that do not have physical meaning. In order to obtain a smoothened hydrograph, we employ the numerical filter introduced by Savitzky and Golay (1964), as shown in Fig. 2a. This filter allows for increasing the signal-to-noise ratio without greatly distorting the signal. This is achieved by replacing the raw data values by new ones, which are computed from a moving polynomial fit to  $2n + 1$  neighbouring points, with  $n$  being at least equal to

the order of the polynomial. When the points are equally spaced (which is the case here, since the time interval is constant, i.e. daily), we obtain an analytical expression, i.e. a symmetric moving average scheme, where the weights (convolution coefficients) of the smoothing procedure are constant. In our context, we employ a 7-point 3rd order polynomial.

- Step (b): We define the beginning and end of the dry period of interest, and its last flow value, as shown in Fig. 2b. First, we seek for the last flow value being greater than  $q_{0j}$  and detect the corresponding date index,  $b_j$ , which denotes the actual beginning of the dry period of year  $j$ . Under this assumption, by using  $q_{0j}$  as cut-off threshold, we ignore the part of the observed hydrograph from April 15th until day  $b_j$ . Next, in order to determine the actual end of the dry period, symbolized  $e_j$ , we calculate the average flows over 15-day intervals and their differences until October 15th. Moving backwards in time, we examine whether the one-step flow trend changes from negative to positive, which marks the end of the dry period,  $e_j$ . Since the number of data points removed from April 15th to the actual beginning of the dry period are  $b_j$ , and the points removed from the actual end of the dry period up to October 15th ( $i = 184$ ) are  $184 - e_j$ , the remaining flow values in the sample, and thus the actual duration of the dry period of year  $j$ , are  $n_j = e_j - b_j + 1$ .
- Step (c): We remove all flow values that lie above the line joining  $q_{0j}$  with  $q_{e_j}$ , which is given by:

$$q_{ij} = q_{0j} - \left( q_{0j} - q'_{e_j} \right) i / (e_j + n_j) \quad (6)$$

where the denominator is the number of days between April 15th and the actual end of the dry period of year  $j$ . All flow values exceeding the theoretical threshold  $q_{ij}$  are removed, since the exponential decay function (3), by definition lies below the line of Eq. (6). As shown in Fig. 2c, the remaining data set is generally discontinuous and contains fewer values than the initial sample of length  $n_j$ , from which all important dry-period flood events have been removed.

- Step (d): We further reduce the remaining flow peaks below the theoretical upper threshold (6), considering small-scale flood events of typical duration up to two days. In this context, we apply a cut-off procedure comprising the identification of the remaining local flow maxima over the dry period, which are next set equal to the value of the previous day. This procedure is repeated only once, to avoid removing a unreasonable number of flow points, thus getting an adjusted flow record containing too few data.

## 2.3 Performance Measure and Associated Benchmarks

In order to evaluate the predictive capacity of the forecasting model against the observed low flows (more accurately, the adjusted flow data), we employ a modified expression of the Nash-Sutcliffe efficiency (NSE), using as benchmark a typical low flow pattern over the dry period, commonly referred to as the *master recession curve*, instead of an average low flow value.

Well-known shortcomings of NSE for hydrological model evaluations have been extensively discussed in the literature (Schaeffli and Gupta 2007; Gupta et al. 2009), including the



case of models for low flow simulations (e.g., Pushpalatha et al. 2012; Nicolle et al. 2014). We remind that NSE compares the mean square error of the modelled flow against the observed data to the variance of the observed data, thus comparing the predictions of the actual model to the predictions provided by the observed mean value; under this premise, a positive efficiency indicates that the model is a better predictor than the observed mean. However, the mean value as the benchmark predictor in the context of low flow evaluations is far from being representative, since the river regime during the dry period exhibits an evident non-stationary behaviour due to the systematic decrease of runoff.

Within calibrations, we initially considered as benchmarks the daily average streamflow curve, as advocated by Garrick et al. (1978) and Martinec and Rango (1989), as well as the daily median streamflow curve, which is generally a better estimator than the mean, because the dry period flows are highly skewed. However, due to noise effects, these two benchmarks (particularly that with the mean) exhibit random fluctuations, which are not desirable (see example in Fig. 3). The reason for that is that the benchmark should normally reflect baseflow and be uninfluenced from extremes in the dataset. To remove fluctuations, we tested three alternative exponential functions, i.e. master recession curves, which were fitted to the daily means and medians, as well as the lower envelope of medians (see example in Fig. 3). The latter, symbolized  $m_i$ , is considered the most representative for the average dry period baseflow, and thus it was finally selected as benchmark within calibrations.

Based on the above assumptions and preliminary results by Risva et al. (2017), the modified NSE function for  $N$  dry period intervals is given by:

$$MNSE = 1 - \frac{\sum_{j=1}^N \sum_{i=b_j}^{e_j} (q_{0j} \exp(-k_j t_i) - q'_{ij})^2}{\sum_{j=1}^N \sum_{i=b_j}^{e_j} (m_i - q'_{ij})^2} \tag{7}$$

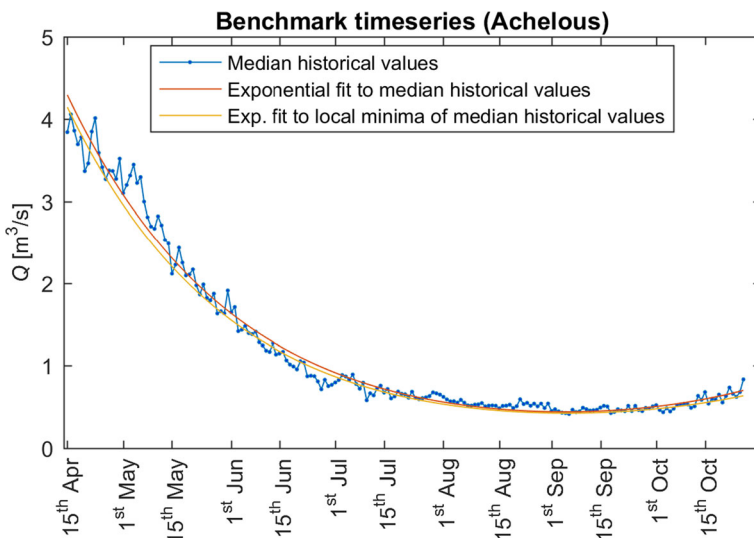


Fig. 3 Example of alternative master recession curves used as benchmark functions, extracted from the observed dry period flow data for Achelous River, Greece

where  $j$  is the dry period index;  $b_j$  and  $e_j$  are the beginning and end day of dry period  $j$ ;  $q'_{ij}$  are the adjusted flow values across the dry period  $j$ ;  $q_{0j}$  is the starting flow (i.e. the lower flow value between April 1st and April 15th of year  $j$ );  $k_j$  is the (unknown) recession parameter of period  $j$ ;  $t_i$  is a day index (integer); and  $m_i$  is the benchmark flow value of day  $i$ , estimated on the basis of the master recession curve for the specific catchment.

We remark that by adopting the classical NSE metric, in the denominator of (7) we would apply a constant benchmark value  $m$ , equal to the average of all adjusted flow values,  $q'_{ij}$ . Obviously, such benchmark would be a highly inaccurate predictor of the low flow dynamics; its use would therefore provide unrealistically high performance scores, thus making it difficult to evaluate the actual predictive capacity of our modelling framework.

## 2.4 Randomly Selected Multiple Subsets Calibration Framework

The calibration problem has been formulated for estimating the “annually varying” (i.e., with a different value for each year) recession coefficients  $k_j$ , in two ways: first by maximizing the criterion of (7) for each specific dry period  $j$  separately, and, second, by maximizing this criterion for all dry periods collectively, which allows for obtaining the “overyear” (basin-specific) parameters  $a$  and  $b$ . Evidently, this is essential for running the model for future conditions, i.e. in forecast mode, using as sole information the initial flow  $q_{0j}$ .

In the second case, for the parameter estimation procedure and its validation, we employed a stochastic approach, to account for the uncertainties induced due to the use of relatively small

**Table 1** Characteristic properties of study basins

No	River	Country	Station name	Elevation (m)	Basin area (km <sup>2</sup> )	Data period*
1	Ebro	Spain	Castejon	265	25,194	1949–2012 (63)
2	Aragon	Spain	Caparosso	302	5469	1950–2013 (63)
3	Jucar	Spain	Cuenca	916	984	1950–2013 (63)
4	Alcanadre	Spain	Lascellas	390	501	1945–2013 (62)
5	Albaida	Spain	Montabemer	162	320	1992–2013 (21)
6	Algas	Spain	Horta de San Juan	418	115	1965–2013 (49)
7	Turia	Spain	Tramacastilla	1278	95	1945–2013 (56)
8	Aude	France	Carcassone	96	1754	1969–2016 (46)
9	Argens	France	Arcs	36	1730	1966–2016 (47)
10	Doux (Rhône)	France	Tournon	127	640	2005–2016 (12)
11	Orbieu	France	Luc	34	586	1969–1998 (19)
12	Lèze	France	Labarthe	159	351	1969–2016 (47)
13	Loup	France	Tourrettes	124	206	1972–2016 (32)
14	Vixiège	France	Belpèch	243	196	1969–2016 (42)
15	Fium-Alto	France (Corsica)	Taglio-Isolaccio	35	114	1961–2016 (40)
16	La Coise	France	Larajasse	571	61	1970–2016 (43)
17	Limnatis	Cyprus	Kouris Dam	277	115	1984–2009 (24)
18	Germasogeia	Cyprus	Foinikaria	100	110	1969–2009 (41)
19	Stavros Psokas	Cyprus	Skarfos	185	78	1985–2009 (25)
20	Peristerona	Cyprus	Panagia Bridge	546	77	1966–2012 (44)
21	Xeros	Cyprus	Lazarides	553	69	1971–2011 (41)
22	Amo	Italy	Subbiano	750	751	1992–2013 (22)
23	Tanaro	Italy	Piantorre	1067	500	2002–2012 (11)
24	Salso	Italy (Sicily)	Petralia	760	28	1954–2003 (33)
25	Achelous	Greece	Kremasta dam	146	3570	1967–2008 (42)

(\*) Complete years, in parentheses

**Table 2** Summary flow statistics for study basins (mm)

No	River	Mean $Q$	St. dev.	$Q_5$	$Q_{25}$	$Q_{50}$	$Q_{75}$	$Q_{95}$
1	Ebro	0.77	0.97	2.60	0.97	0.40	0.20	0.11
2	Aragon	0.87	1.27	3.29	0.99	0.40	0.19	0.09
3	Jucar	0.81	1.21	2.50	0.92	0.47	0.23	0.10
4	Alcanadre	0.72	1.26	2.46	0.77	0.35	0.18	0.09
5	Albaida	0.21	0.38	0.55	0.23	0.14	0.09	0.03
6	Algas	0.57	3.04	1.79	0.36	0.13	0.05	0.01
7	Turia	0.67	0.74	1.75	0.87	0.45	0.27	0.12
8	Aude	0.95	1.24	2.54	1.18	0.62	0.35	0.18
9	Argens	0.57	0.89	1.88	0.61	0.28	0.17	0.09
10	Doux (Rhône)	1.15	2.40	3.81	1.25	0.59	0.17	0.02
11	Orbieu	0.75	1.86	2.76	0.78	0.25	0.08	0.01
12	Lèze	0.47	1.10	1.75	0.48	0.15	0.05	0.02
13	Loup	1.52	2.47	5.36	1.65	0.73	0.36	0.16
14	Vixiège	0.53	1.54	2.07	0.52	0.11	0.03	0.01
15	Fium-Alto	1.04	2.87	3.07	0.93	0.44	0.23	0.11
16	La Coise	0.89	1.41	2.86	1.12	0.48	0.17	0.04
17	Limnatis	0.34	0.99	1.35	0.35	0.10	0.00	0.00
18	Germasogcia	0.38	1.23	1.60	0.36	0.08	0.00	0.00
19	Stavros Psokas	0.21	0.64	0.99	0.16	0.01	0.00	0.00
20	Peristerona	0.42	1.53	1.70	0.35	0.06	0.00	0.00
21	Xeros	0.35	0.89	1.45	0.26	0.09	0.06	0.03
22	Arno	1.37	2.97	5.00	1.37	0.56	0.17	0.06
23	Tanaro	1.79	3.41	4.76	2.06	1.04	0.48	0.23
24	Salso	2.40	8.35	9.65	1.74	0.40	0.06	0.00
25	Achelous	2.61	3.48	7.87	3.37	1.53	0.65	0.34

samples. It is well-known that a shortcoming of the classical calibration-validation paradigm, referred to as split-sample test (Klemeš 1986), is the dependency of the model performance and the optimized parameters on the length and time window of the used data sample (Gharari et al. 2013). To account for the associated uncertainties, we repeated the calibration-validation procedure 1000 times. At each trial, we randomly split the whole data set into calibration and validation sub-sets (not necessarily with contiguous time intervals), containing 80 and 20% of dry period intervals respectively. Using this approach, also regarded as heuristic multiobjective calibration (Efstratiadis and Koutsoyiannis 2010), we obtained 1000 sets of parameter values and the associated performance metrics in calibration and validation (see section 4.2).

### 3 Study Areas

We have collected daily flow data from 25 Mediterranean catchments from Spain (7), France (9), Cyprus (5), Italy (3) and Greece (1), which were mainly obtained from online databases. For these catchments, key properties and summary hydrological statistics, in the form of flow quantiles, are given in Tables 1 and 2, respectively. As shown, the study areas cover a wide range of hydrological characteristics, in terms of basin area, mean ground elevation and runoff production, including some small catchments with intermittent flow regime. The station sites are illustrated on the map of Fig. 4. For convenience, all flow time series were converted into equivalent water depths ( $\text{mm d}^{-1}$ ), to allow direct comparisons across basins of different size. In this context, the initial discharge,  $q_0$ , and parameter  $a$  in eq. (4) will hereafter be referred to  $\text{mm d}^{-1}$  and  $\text{mm}^{-1}$ , respectively.



**Fig. 4** Map of examined stations; station names are listed in Table 1

The largest basin is Ebro, Spain, upstream of Castejon station, which extends over an area of more than 25,000 km<sup>2</sup>. On the other hand, the smallest catchment is Salso (tributary of Imera Meridionale), Sicily, upstream of Petralia station, the area of which is only 28 km<sup>2</sup>. The range of mean ground elevations is also large, from headwater mountainous catchments to low elevation coastal ones. Regarding the runoff production, we investigate from very wet basins, such as Achelous, Greece, with a mean daily runoff of 2.61 mm d<sup>-1</sup> (more than 950 mm y<sup>-1</sup>), to very dry ones, such as Albaida (Spain) and Stavros tis Psokas (Cyprus), which produce only 0.21 mm d<sup>-1</sup>, on average (75 mm y<sup>-1</sup>).

## 4 Results and Discussion

### 4.1 Assessment and Interpretation of Annually Varying Recession Rates

For each catchment, we initially calculated the median value of the reference time horizon (April 15th to October 15th), on the basis of which we extracted the master recession curve, to be used next as benchmark low flow data within calibrations. We also estimated the average dry period duration and its median flow, which are characteristic indices of the hydrological behaviour of the studied catchments during the low flow period (Table 3). We remark that in some catchments with intermittent flow, the length of the low flow period is lower than expected (e.g. 115 days, in the catchment called Stavros tis Psokas, Cyprus) because conventionally, the end of the dry period is marked by the point of inflection of the master recession curve. Therefore, even a minor flood flow is assumed as indicator of the beginning of the next wet period.

Next, for each year  $j$ , we estimated the initial discharge,  $q_{0j}$ , i.e., the minimum daily flow between 1st and 15th April, and solved a one-dimensional optimization problem to infer,

**Table 3** Recession analysis results, considering annually varying recession coefficients

No	Aver. dry period duration (d)	Median $Q_{dry}$ (mm)	Mean MNSE	Recession coefficient, $k$ ( $d^{-1}$ )			Initial discharge, $q_0$ (mm)			Correl. $k$ vs $q_0$
				Mean	Median	St. dev.	Mean	Median	St. dev.	
1	128	0.25	0.663	0.0121	0.0118	0.0068	0.69	0.58	0.45	0.674
2	135	0.29	0.751	0.0173	0.0093	0.0327	0.62	0.49	0.49	0.039
3	172	0.37	0.791	0.0095	0.0093	0.0044	0.85	0.80	0.54	0.419
4	152	0.25	0.739	0.0130	0.0097	0.0124	0.48	0.41	0.32	0.227
5	130	0.11	0.781	0.0172	0.0108	0.0248	0.17	0.13	0.12	-0.117
6	195	0.08	0.740	0.0177	0.0145	0.0208	0.35	0.19	0.41	-0.011
7	141	0.09	0.794	0.0122	0.0108	0.0077	1.05	0.89	0.79	-0.175
8	167	0.50	0.684	0.0084	0.0081	0.0029	1.05	0.94	0.56	0.759
9	143	0.24	0.840	0.0076	0.0070	0.0035	0.51	0.37	0.38	0.588
10	150	0.22	0.705	0.0218	0.0218	0.0125	0.74	0.60	0.40	-0.179
11	195	0.14	0.654	0.0197	0.0163	0.0112	0.70	0.71	0.47	0.165
12	159	0.08	0.701	0.0185	0.0184	0.0076	0.36	0.33	0.22	0.263
13	143	0.51	0.781	0.0118	0.0124	0.0055	1.12	0.99	0.63	0.595
14	195	0.04	0.629	0.0267	0.0213	0.0350	0.44	0.42	0.30	0.459
15	147	0.28	0.619	0.0132	0.0131	0.0062	0.96	0.89	0.76	0.633
16	147	0.24	0.646	0.0183	0.0168	0.0097	0.58	0.48	0.37	0.263
17	186	0.00	0.804	0.0391	0.0337	0.0192	0.38	0.28	0.28	-0.513
18	195	0.01	0.729	0.0347	0.0293	0.0262	0.40	0.29	0.33	-0.257
19	115	0.00	0.799	0.0393	0.0366	0.0098	0.19	0.12	0.14	-0.098
20	155	0.00	0.734	0.0346	0.0326	0.0102	0.30	0.26	0.16	-0.275
21	149	0.06	0.443	0.0158	0.0153	0.0063	0.29	0.24	0.20	0.648
22	140	0.21	0.558	0.0191	0.0183	0.0069	0.92	0.89	0.53	0.778
23	162	0.67	0.734	0.0123	0.0117	0.0041	1.60	1.21	0.90	0.593
24	122	0.35	0.698	0.0294	0.0294	0.0166	0.79	0.73	0.41	0.235
25	144	0.80	0.485	0.0130	0.0131	0.0044	2.67	2.58	1.10	0.870

through calibration, the recession rate,  $k_j$ , of the corresponding dry period, using as performance measure the adjusted low flow data and the MNSE metric of Eq. (7). As shown in Table 4, in all basins, the fitting of the linear reservoir approach by Eq. (3) is very good, with few exceptions that are related to peculiar hydrological conditions during specific periods (e.g., too late start of the dry period  $j$ , thus making  $q_{0j}$  unsuitable for low flow predictions).

The key statistics of the two variables of interest, i.e.  $k_j$  and  $q_{0j}$ , as well as their Pearson correlation coefficient are summarized in Table 3. All the aforementioned quantities exhibit significant variability across catchments. It is noteworthy to mention that in some basins  $k_j$  and  $q_{0j}$  are strongly correlated (e.g., 0.87 in Achelous), thus indicating that the variation of the recession rate is well explained by the variation of  $q_{0j}$ , representing the basin state at the end of the wet period. However, in other areas the correlation is very low (even negative), which means that the low flow dynamics does not depend on the catchment conditions at the conventional end of the wet period, i.e. early April.

In order to further explain the spatial variability of the recession coefficient, we also calculated its correlation with the typical flow statistics of Table 2 and some other indices. In Fig. 5, we provide scatter plots of the median value of  $k_j$  (next symbolized  $k$ ) against four indices, i.e.  $Q_{dry}/Q_{50}$ ,  $Q_{dry}/Q_0$ ,  $Q_{dry}/Q_{25}$  and  $Q_{50}/Q_{25}$ , where  $Q_{dry}$  is the median flow value across all dry periods (Table 3). The highest correlation (apparently negative) is between  $k$  and  $Q_{dry}/Q_{25}$ , which shows that the recession coefficient is associated with the “distance” of these two runoff characteristics.

**Table 4** Average values of regional parameters  $a$  and  $b$ , and average performance indices resulting from the Randomly Selected Multiple Subsets (RSMs) calibration framework for 1000 random calibration/validation sets

No	Name	$a$ (d <sup>-1</sup> )	$b$ (mm d <sup>-1</sup> )	MNSE		NSE	
				Calibration	Validation	Calibration	Validation
1	Ebro	0.010	0.004	0.582	0.543	0.805	0.790
2	Aragon	0.012	0.001	0.374	0.266	0.683	0.623
3	Jucar	0.004	0.005	0.579	0.437	0.789	0.742
4	Alcanadre	0.008	0.007	0.589	0.464	0.895	0.859
5	Albaida	0.009	0.007	0.659	0.487	0.842	0.755
6	Algas	0.005	0.013	0.762	0.718	0.967	0.957
7	Turia	-0.001	0.011	0.591	0.289	0.732	0.553
8	Aude	0.003	0.005	0.541	0.456	0.873	0.861
9	Argens	0.002	0.007	0.793	0.722	0.877	0.855
10	Doux (Rhône)	0.001	0.019	0.593	0.354	0.928	0.891
11	Orbieu	-0.001	0.019	0.429	-0.235	0.710	0.553
12	Lèze	-0.001	0.020	0.739	0.692	0.948	0.942
13	Loup	0.002	0.010	0.591	0.531	0.908	0.886
14	Vixiège	0.022	0.012	0.474	0.373	0.877	0.853
15	Fium-Alto	0.004	0.009	0.755	0.607	0.884	0.851
16	La Coise	0.009	0.011	0.640	0.594	0.935	0.930
17	Limnatis	-0.003	0.031	0.866	0.831	0.909	0.884
18	Germasogeia	0.007	0.022	0.868	0.848	0.916	0.901
19	Stavros Psokas	0.003	0.037	0.890	0.871	0.932	0.915
20	Peristerona	-0.016	0.039	0.732	0.702	0.875	0.868
21	Xeros	0.016	0.011	0.804	0.720	0.888	0.862
22	Arno	0.011	0.009	0.554	0.456	0.920	0.910
23	Tanaro	0.002	0.009	0.606	0.453	0.939	0.895
24	Salso	0.008	0.015	0.414	0.359	0.757	0.731
25	Achelous	0.003	0.005	0.524	0.474	0.902	0.898

Another characteristic associated with the median recession rate,  $k$ , is the catchment area,  $A$ . As shown in Fig. 6,  $k$  is well correlated with  $A^{-1/2}$ . Actually, the increase of  $k$  with the decrease of the basin area is consistent with the theoretical background of the linear recession model, which is the Boussinesq equation (Eng and Milly 2007). It is interesting to remark that in the scatter plot of Fig. 6, two clearly different clusters of catchments are recognized. However, we did not find any interpretation of this classification on the basis of hydrological indices or any other information extracted from our data set. An evident hypothesis is that the two clusters contain catchments with common geological characteristics, by means of porosity and hydraulic conductivity, as anticipated by the Boussinesq theory. We remark that several studies (e.g., Zecharias and Brutsaert 1988; Peña-Arancibia et al. 2010; Li et al. 2018) found that the baseflow recession coefficient is associated with climatic and geomorphological properties (e.g., terrain slope, river network density); however, such information was not available in our case.

#### 4.2 Estimation of Basin-Specific Parameters $a$ and $b$

As indicated by the above analysis, at least in some of the test catchments, the recession rate exhibits quite significant linear correlation with the initial flow; thus the local value of  $k_j$  can be approximated as function of  $q_{0j}$  (Eq. 4). We can therefore accept Eq. (5), assuming that the baseflow recession of each dry period is estimated as function of the initial flow  $q_{0j}$ , representing the hydrological conditions at the end of the wet period, and the two regional (i.e., basin-specific) parameters,  $a$  and  $b$ .

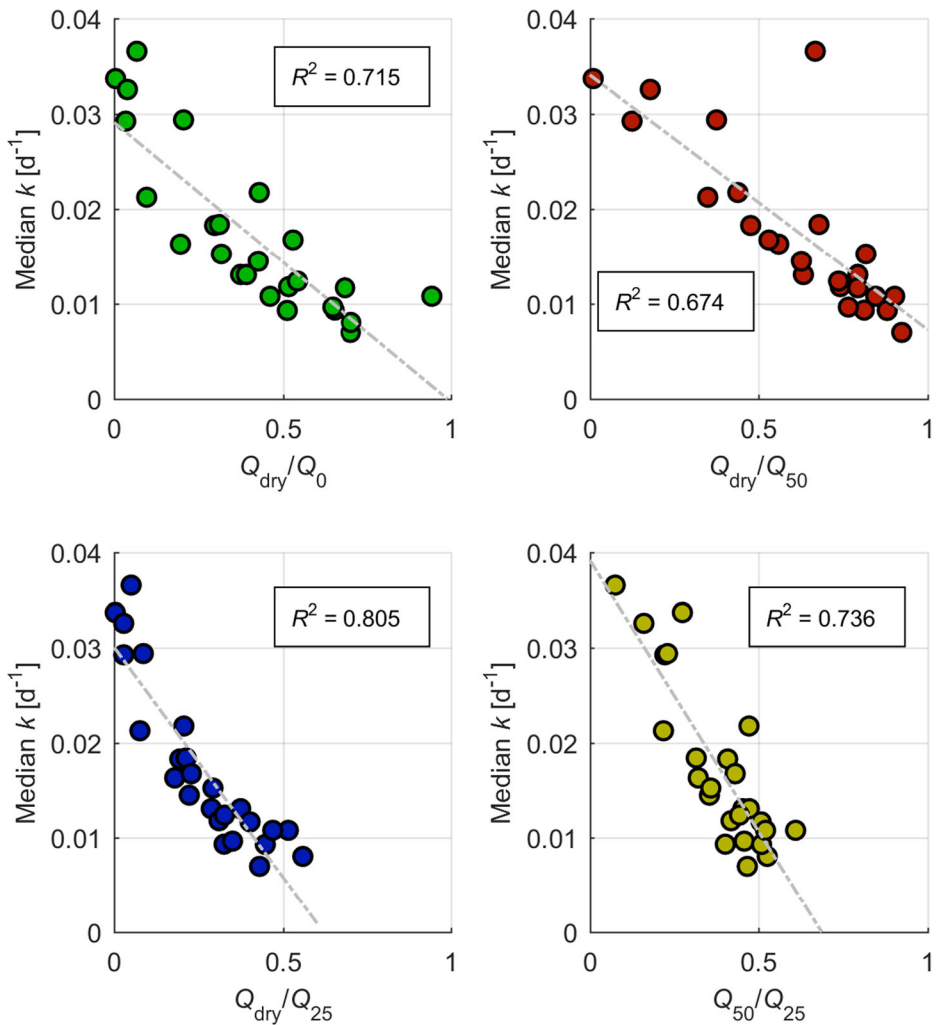


**Fig. 5** Scatter plots of median recession rate against characteristic hydrological indices across the examined catchments

For the estimation of parameters  $a$  and  $b$  for each of the 25 catchments we followed the stochastic calibration framework of section 2.4, resulting in a sample of 1000 optimized parameters and the associated performance metrics in calibration and validation. In Table 4 we display the key results of the analyses, by means of average values of the aforementioned parameters. As illustrated by the MNSE metric, the calibration is very satisfactory in most of the basins, ranging from 0.374 (Aragon) to 0.890 (Stavros Psokas), while in 21 out of the 25 catchments, the MNSE in calibration exceeds 0.50. The predictive capacity of the model is quantified by the validation MNSE score, which, in most basins, is slightly lower than the score in calibration, as expected. Only in one case, i.e. in Orbieu river, the model exhibits unsatisfactory performance, as indicated by the negative MNSE in validation. However, we remind that this metric is very conservative, and if we use the typical NSE (i.e. by considering the average flow across all dry periods as benchmark model), the corresponding validation

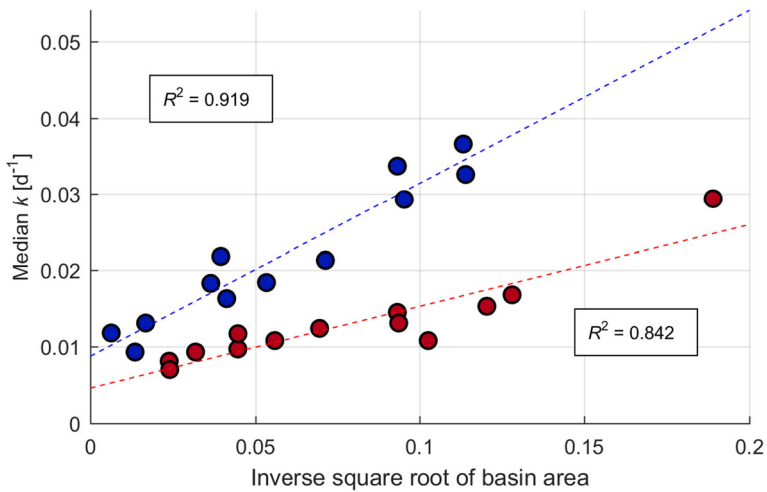


**Fig. 6** Scatter plots of median recession rate against the inverse square root area of the examined catchments

score goes up to 0.55. In general, all NSE values are significantly higher than those of MNSE. Actually, the NSE values in validation exceed 0.80 in 20 out of 25 basins.

In Fig. 7 we show the box plots for parameters  $a$  and  $b$ , on the basis of 1000 optimized values. In most catchments, their variability is generally low, which is a strong evidence of the robustness of the proposed modelling framework. Therefore, the model predictive capacity is not severely influenced by the specific calibration sample. Yet, some basins (e.g. Orbieu) exhibit quite large parameter variability, which is reflected on occasional failure of the forecasting model to reproduce the low flow behaviour during specific dry periods.

The operational version of the forecasting model of each test basin is constructed by considering the average values of  $a$  and  $b$ , which are given in Table 4. Characteristic examples of model fitting for 8 out of 25 basins, and specific dry periods, are given in Fig. 8.

## 5 Conclusions

In Mediterranean catchments (and areas with similar hydroclimatic conditions all over the globe), the dry period is of long duration (up to six months) and is dominated by low flows, as the major, and relatively well predictable, part of the available water resources. Evidently, the earlier and more accurate the prediction of low flow is (over the forthcoming dry period), the more assistance is provided to water resources planners and managers.

Most literature approaches for low flow prediction are valid for wet climates and short forecasting horizons (e.g. a few days), since the dry-period flow regime in such climates is significantly affected by flood events. As a result, in these conditions, extending forecasting horizons up to six month or so would require using ensemble meteorological predictions, which are still highly uncertain and their operational applicability is questionable.

In contrast to the existing approaches, we have developed a simple and parsimonious methodology for predicting low flows up to six months ahead, which was validated on the basis of daily flow data retrieved from 25 Mediterranean rivers, with substantially different characteristics. The proposed method uses the traditional linear reservoir concept under two



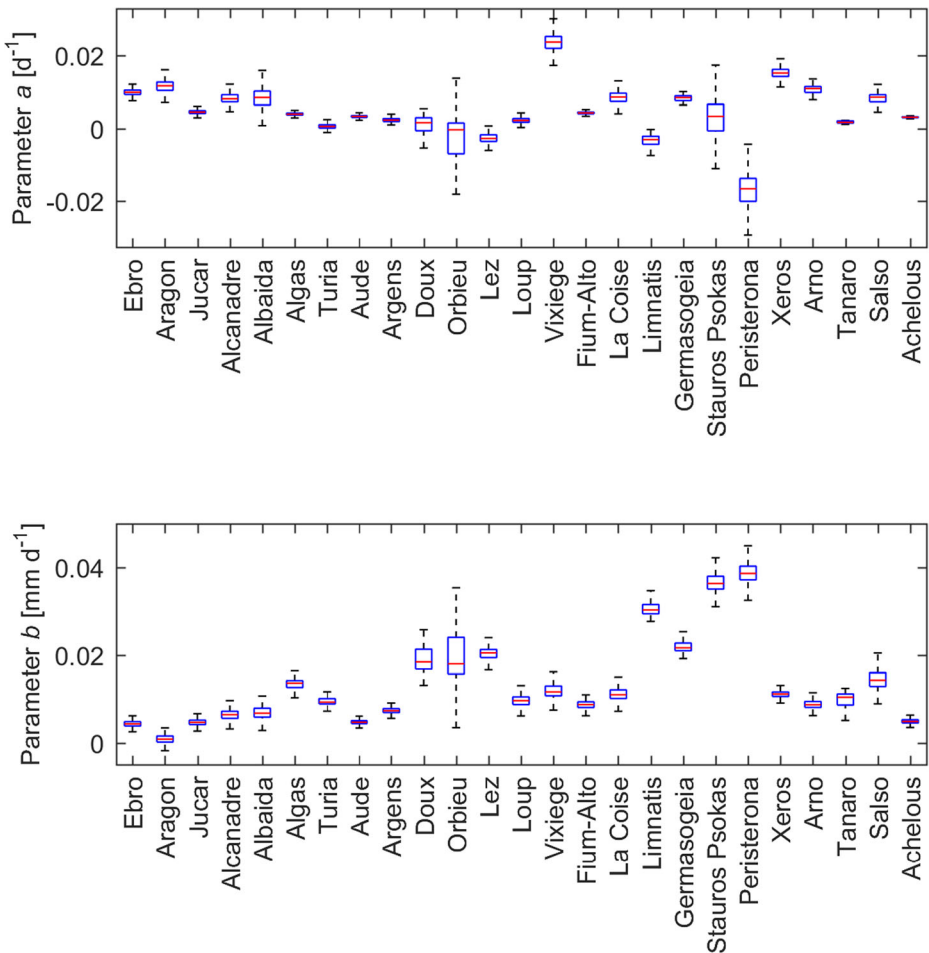
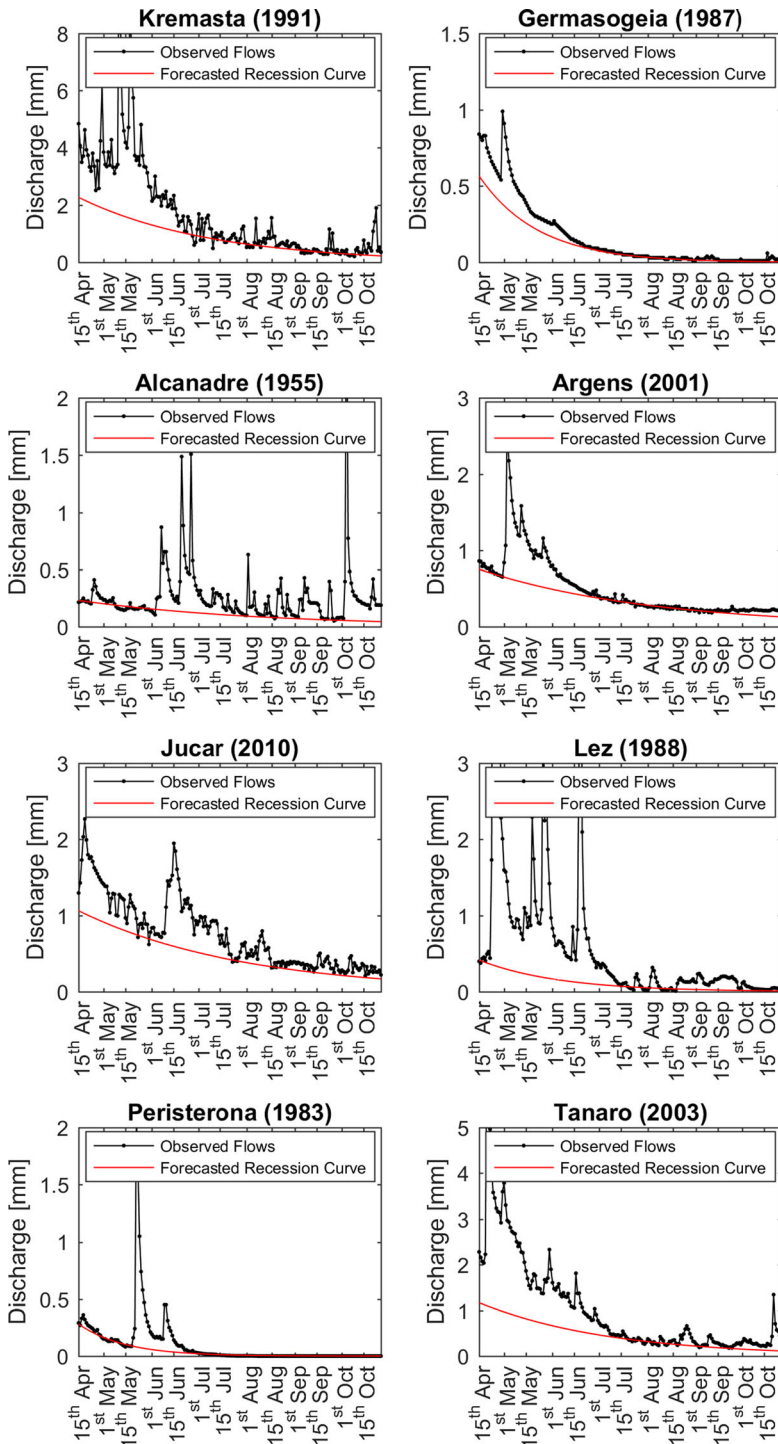


Fig. 7 Box plots of parameters  $a$  and  $b$

main assumptions: assigning as starting flow,  $q_0$ , the minimum flow value during the first two weeks of April, and expressing the annually-varying recession rate  $k$  as a function of  $q_0$  (Eq. (4)). This empirical relationship comprises two site-specific parameters,  $a$  and  $b$ , for the estimation of which we have developed a stochastic methodological framework comprising three major novelties.

The first novelty involves the extraction of the so-called “adjusted flows” during each dry period, by employing consequent filtering and data removal procedures to the original time series. The objective is to determine the actual beginning and end of the dry period, and remove flood peaks and high flow pulses that are due to rainfall events, which provides a flow record that is representative of the low flow dynamics of each specific period.

The second novelty refers to the development of a new metric for the evaluation of the predictive capacity of low-flow models, called modified Nash-Sutcliffe efficiency (Eq. 7). Its necessity rises from the fact that the typical efficiency metric is too favourable, since it uses as benchmark model the average value of the observed data, which is far from being representative and may provide a misleading picture of model fitting. Instead of this naïve benchmark,



**Fig. 8** Examples of forecasted low flows against the observed hydrographs over the conventional reference period (April 15th to October 15th)

we employ a master recession curve constructed by passing a lower envelope curve to the median flow values across the dry period.

The third novelty is a stochastic configuration of the classical split-sample test (i.e., the inference of the unknown model parameters through optimization during a calibration period, and its evaluation against an independent data set in validation), which is the working paradigm in hydrological model calibrations. The proposed procedure, termed Randomly Selected Multiple Subset (RSMS) calibration, retains the key concepts of calibration and validation, yet the distinction of the two periods is not strict. In contrast, a large number of calibration-validation tests are employed, by randomly changing the corresponding data sets. The outcome of the RSMS approach is a large number of alternative optimal parameter sets and related performance metric values, which also allows for evaluating the parameter uncertainty. We remark that the new procedure can be of general use, although here this is exclusively applied for the extraction of the forecasting model parameters,  $a$  and  $b$ .

Extended low flow analyses across the 25 Mediterranean rivers proved that the linear reservoir approach, with recession parameters that are fitted to the adjusted low flow data of each dry period, ensures very good model performance. As expected, the variability of the recession rate across dry periods is significant, and in several cases it proved to be associated with the hydrological conditions at the end of the antecedent wet period. The median of the recession coefficients is also significantly varying across catchments, and this variability is well explained by typical hydrological indices, particularly the ratios  $Q_{\text{dry}}/Q_{25}$  and  $Q_{50}/Q_{25}$ , where  $Q_{\text{dry}}$  is the median flow value across all dry periods and  $Q_{25}$  is the 25% percentile of daily flow data.

An interesting outcome is that the median recession coefficient is inversely proportional to the square root of the catchment area. This is consistent with the Boussinesq equation, which is the theoretical basis of the linear recession model. With regard to this relationship two distinct clusters of catchments were clearly recognized; however, more information is required in order to explain this behaviour.

Finally, by employing the RSMS calibration procedure, we extracted the parameters of the low flow forecasting model, as well as the associated performance metrics, and evaluated their uncertainty using randomly selected calibration-validation samples. Overall, the results are very encouraging, thus making it possible to employ the average parameter values within Eq. (5) for estimating the evolution of the baseflow component during each dry period, using, as sole input, the observed flow data at the end of the preceding wet period. Actually, provided that the basin-specific parameters are known, a few flow measurements (or even a single measurement) at mid-April may be sufficient, which makes the proposed tool very attractive for areas with limited sources of hydrometric observations.

**Acknowledgments** A previous shorter version of the paper, including the key components of the methodology and preliminary results from four out of 25 basins, has been presented in the *10th World Congress of EWRA "Panta Rhei" Athens, Greece, 5-9 July 2017*, under the title "A simple model for low flow forecasting in Mediterranean streams" (Risva et al. 2017). The authors are grateful to the fruitful comments by the Guest Editor of *Water Resources Management* and the anonymous reviewer, which helped improve the initial version of this article significantly.

## Compliance with Ethical Standards

**Conflict of Interest** None.

## References

- Aksoy H, Wittenberg H (2011) Nonlinear baseflow recession analysis in watersheds with intermittent streamflow. *Hydrol Sci J* 56(2):226–237. <https://doi.org/10.1080/02626667.2011.553614>
- Akylas E, Gravanis E, Koussis AD (2015) Quasi-steady flow in sloping aquifers. *Water Resour Res* 51(11): 9165–9181. <https://doi.org/10.1002/2014WR016651>
- Anderson M, Burt T (1980) Interpretation of recession flow. *J Hydrol* 46(1–2):89–101. [https://doi.org/10.1016/0022-1694\(80\)90037-2](https://doi.org/10.1016/0022-1694(80)90037-2)
- Aschwanden H, Kan C (1999) Le débit d'étiage Q347—Etat de la question. *Communications hydrologiques* 27. Service Hydrol. et Géol. National, Berne
- Assani AA, Chalifour A, Légaré G, Manouane C-S, Leroux D (2011) Temporal regionalization of 7-day low flows in the St. Lawrence watershed in Quebec (Canada). *Water Resour Manag* 25(14):3559. <https://doi.org/10.1007/s11269-011-9870-6>
- Boussinesq J (1903) Sur le de'bit, en temps de sécheresse, d'une source alimentée par une nappe d'eaux d'infiltration. *C R Acad Sci* 136:1511–1517
- Brandes D, Hoffmann JG, Mangarillo JT (2005) Base flow recession rates, low flows, and hydrologic features of small watersheds in Pennsylvania, USA. *J Am Water Resour Assoc* 41:1177–1186. <https://doi.org/10.1111/j.1752-1688.2005.tb03792.x>
- Brutsaert W, Nieber JL (1977) Regionalized drought flow hydrographs from a mature glaciated plateau. *Water Resour Res* 13(3):637–643. <https://doi.org/10.1029/WR013i003p00637>
- Castiglioni S, Castellarin A, Montanari A (2009) Prediction of low-flow indices in ungauged basin through physiographical space-based interpolation. *J Hydrol* 378:272–280. <https://doi.org/10.1016/j.jhydrol.2009.09.032>
- Castiglioni S, Castellarin A, Montanari A, Skøien JO, Laaha G, Blöschl G (2011) Smooth regional estimation of low-flow indices: physiographical space based interpolation and top-kriging. *Hydrol Earth Syst Sci* 15:715–727. <https://doi.org/10.5194/hess-15-715-2011>
- Cervi F, Blöschl G, Corsini A, Borgatti L, Montanari A (2017) Perennial springs provide information to predict low flows in mountain basins. *Hydrol Sci J* 62(15):2469–2481. <https://doi.org/10.1080/02626667.2017.1393541>
- Demirel MC, Booiij MJ, Hoekstra AY (2013) Effect of different uncertainty sources on the skill of 10 day ensemble low flow forecasts for two hydrological models. *Water Resour Res* 49:4035–4053. <https://doi.org/10.1002/wrcr.20294>
- Demirel MC, Booiij MJ, Hoekstra A (2015) The skill of seasonal ensemble low-flow forecasts in the Moselle River for three different hydrological models. *Hydrol Earth Syst Sci* 19:275–291. <https://doi.org/10.5194/hess-19-275-2015>
- Efstratiadis A, Koutsoyiannis D (2010) One decade of multiobjective calibration approaches in hydrological modelling: a review. *Hydrol Sci J* 55(1):58–78. <https://doi.org/10.1080/02626660903526292>
- Eng K, Milly PCD (2007) Relating low-flow characteristics to the base flow recession time constant at partial record stream gauges. *Water Resour Res* 43(1):W01201. <https://doi.org/10.1029/2006WR005293>
- Engeland K, Hisdal H (2009) A comparison of low flow estimates in ungauged catchments using regional regression and the HBV-model. *Water Resour Manag* 23:2567–2586. <https://doi.org/10.1007/s11269-008-9397-7>
- Eslamian S, Ghasemzadeh M, Biabanaki M, Talebizadeh M (2010) A principal component regression method for estimating low flow index. *Water Resour Manag* 24:2553–2566. <https://doi.org/10.1007/s11269-009-9567-2>
- Farahani MA, Khalili D (2013) Seasonality characteristics and spatio-temporal trends of 7-day low flows in a large, semi-arid watershed. *Water Resour Manag* 27(14):4897. <https://doi.org/10.1007/s11269-013-0445-6>
- Fiorotto V, Caroni E (2013) A new approach to master recession curve analysis. *Hydrol Sci J* 58(5):966–975. <https://doi.org/10.1080/02626667.2013.788248>
- Garrick M, Cumane C, Nash JE (1978) A criterion of efficiency for rainfall-runoff models. *J Hydrol* 36:375–381. [https://doi.org/10.1016/0022-1694\(78\)90155-5](https://doi.org/10.1016/0022-1694(78)90155-5)
- Gharari S, Hrachowitz M, Fenicia F, Savenije HHG (2013) An approach to identify time consistent model parameters: sub-period calibration. *Hydrol Earth Syst Sci* 17:149–161. <https://doi.org/10.5194/hess-17-149-2013>
- Gottschalk L, Tallaksen LM, Perzyna G (1997) Derivation of low flow distribution functions using recession curves. *J Hydrol* 194(1–4):239–262. [https://doi.org/10.1016/S0022-1694\(96\)03214-3](https://doi.org/10.1016/S0022-1694(96)03214-3)
- Gupta HV, Kling H, Yilmaz KK, Martinez GV (2009) Decomposition of the mean squared error and NSE performance criteria: Implications for improving hydrological modelling. *J Hydrol* 377:80–91. <https://doi.org/10.1016/j.jhydrol.2009.08.003>

- Gustard A, Bullock A, Dixon JM (1992) Low flow estimation in the United Kingdom. Institute of Hydrology, Wallingford, Report No. 108, 88 pp, append
- Hall FR (1968) Base-flow recessions – a review. *Water Resour Res* 4(5):973–983. <https://doi.org/10.1029/WR004i005p00973>
- Institute of Hydrology (1980) Low flow studies. Wallingford
- Jenicek M, Seibert J, Zappa M, Staudinger M, Jonas T (2016) Importance of maximum snow accumulation for summer low flows in humid catchments. *Hydrol Earth Syst Sci* 20:859–874. <https://doi.org/10.5194/hess-20-859-2016>
- Klemeš V (1986) Operational testing of hydrological simulation models. *Hydrol Sci J* 31(1):13–24. <https://doi.org/10.1080/02626668609491024>
- Kroll C, Luz J, Allen B, Vogel R (2004) Developing a watershed characteristics database to improve low streamflow prediction. *J Hydrol Eng* 9(2):116–125. [https://doi.org/10.1061/\(ASCE\)1084-0699\(2004\)9:2\(116\)](https://doi.org/10.1061/(ASCE)1084-0699(2004)9:2(116))
- Laaha G, Blöschl G (2006a) A comparison of low flow regionalisation methods – catchment grouping. *J Hydrol* 323(1–4):193–214. <https://doi.org/10.1016/j.jhydrol.2005.09.001>
- Laaha G, Blöschl G (2006b) Seasonality indices for regionalizing low flows. *Hydrol Process* 20(18):3851–3878. <https://doi.org/10.1002/hyp.6161>
- Laaha G, Blöschl G (2007) A national low flow estimation procedure for Austria. *Hydrol Sci J* 52(4):625–644. <https://doi.org/10.1623/hysj.52.4.625>
- Laaha G, Demuth S, Hisdal H, Kroll CN, van Lanen HAJ, Nester T, Rogger M, Sauquet E, Tallaksen LM, Woods RA, Young A (2013) Prediction of low flows in ungauged basins. In: Blösch G, Sivapalan M, Wagener T, Viglione A, Savenije H (eds) *Runoff Predictions in Ungauged Basins*. Cambridge University Press, Cambridge, pp 163–188
- Li Q, Wei X, Yang X, Giles-Hansen K, Zhang M, Liu W (2018) Topography significantly influencing low flows in snow-dominated watersheds. *Hydrol Earth Syst Sci* 22:1947–1956. <https://doi.org/10.5194/hess-22-1947-2018>
- Longobardi A, Vallini P (2008) Baseflow index regionalization analysis in a Mediterranean area and data scarcity context: role of the catchment permeability index. *J Hydrol* 355(1–4):63–75. <https://doi.org/10.1016/j.jhydrol.2008.03.011>
- Ludwig AH, Tasker GD (1993) Regionalization of low-flow characteristics of Arkansas streams. USGS Water Resources Investigations Report:93, 19 pp–4013
- Maillet E (1905) *Essai d'Hydraulique Souterraine et Fluviale*. Paris, Hermann, Librairie scientifique
- Martinez J, Rango A (1989) Merits of statistical criteria for the performance of hydrological models. *Water Resour Bull* 25(2):421–432. <https://doi.org/10.1111/j.1752-1688.1989.tb03079.x>
- Mehaiguen M, Meddi M, Longobardi A, Toumi S (2012) Low flows quantification and regionalization in North West Algeria. *J Arid Environ* 87:67–76. <https://doi.org/10.1016/j.jaridenv.2012.07.014>
- Merheb M, Moussa R, Abdallah C, Colin F, Perrin C, Baghdadi N (2016) Hydrological response characteristics of Mediterranean catchments at different time scales: a meta-analysis. *Hydrol Sci J* 61(14):2520–2539. <https://doi.org/10.1080/02626667.2016.1140174>
- Nicolle P, Pushpalatha R, Perrin C, François D, Thiéry D, Mathevet T, Le Lay M, Besson F, Soubeyroux JM, Viel C, Regimbeau F, Andréassian V, Maugis P, Augéard B, Morice E (2014) Benchmarking hydrological models for low-flow simulation and forecasting on French catchments. *Hydrol Earth Syst Sci* 18:2829–2857. <https://doi.org/10.5194/hess-18-2829-2014>
- Ouarda TBMJ, Charron C, St-Hilaire A (2008) Statistical models and the estimation of low flows. *Canad Water Resour J* 33(2):195–206. <https://doi.org/10.4296/cwrj3302195>
- Peña-Arancibia JL, van Dijk AIJM, Mulligan M, Bruijnzeel LA (2010) The role of climatic and terrain attributes in estimating baseflow recession in tropical catchments. *Hydrol Earth Syst Sci* 14:2193–2205. <https://doi.org/10.5194/hess-14-2193-2010>
- Pushpalatha R, Perrin C, Le Moine N, Andréassian V (2012) A review of efficiency criteria suitable for evaluating low-flow simulations. *J Hydrol* 420–421:171–182. <https://doi.org/10.1016/j.jhydrol.2011.11.055>
- Risva K, Nikolopoulos D, Efstratiadis A, Nalbantis I (2017) A simple model for low flow forecasting in Mediterranean streams. *European Water* 57:337–343
- Rupp DE, Selker JS (2006) Information, artifacts, and noise in dQ/dt-Q recession analysis. *Adv Water Resour* 29:154–160. <https://doi.org/10.1016/j.advwatres.2005.03.019>
- Savitzky A, Golay MJE (1964) Smoothing and differentiation of data by simplified least squares procedures. *Anal Chem* 36(8):1627–1639. <https://doi.org/10.1021/ac60214a047>
- Schaefli B, Gupta HV (2007) Do Nash values have value? *Hydrol. Processes* 21(15):2075–2080. <https://doi.org/10.1002/hyp.6825>
- Schreiber P, Demuth S (1997) Regionalisation of low flows in southwest Germany. *Hydrol Sci J* 42(6):845–858. <https://doi.org/10.1080/02626669709492083>

- Singh KP, Stall JB (1971) Derivation of base flow recession curves and parameters. *Water Resour Res* 7(2):292–303. <https://doi.org/10.1029/WR007i002p00292>
- Smakhtin VU (2001) Low flow hydrology: a review. *J Hydrol* 240(3–4):147–186. [https://doi.org/10.1016/S0022-1694\(00\)00340-1](https://doi.org/10.1016/S0022-1694(00)00340-1)
- Smakhtin VU, Watkins DA, Hughes DA (1995) Preliminary analysis of low-flow characteristics of South African rivers. *Water SA* 21(3):201–210
- Stoelzle M, Stahl K, Weiler M (2013) Are streamflow recession characteristics really characteristic? *Hydrol Earth Syst Sci* 17:817–828. <https://doi.org/10.5194/hess-17-817-2013>
- Štravs L, Brilly M (2007) Development of a low-flow forecasting model using the M5 machine learning method. *Hydrol Sci J* 52(3):466–477. <https://doi.org/10.1623/hysj.52.3.466>
- Tallaksen L (1995) A review of baseflow recession analysis. *J Hydrol* 165(1–4):349–370. [https://doi.org/10.1016/0022-1694\(94\)02540-R](https://doi.org/10.1016/0022-1694(94)02540-R)
- Tsakiris G, Nalbantis I, Cavadias G (2011) Regionalization of low flows based on Canonical Correlation Analysis. *Adv Water Resour* 34(7):865–872. <https://doi.org/10.1016/j.advwatres.2011.04.007>
- Vafakhah M, Eslamian S, Khosrobeigi Bozchaloei S (2014) Low-flow hydrology. In: *Handbook of Engineering Hydrology: Fundamentals and Applications*, Eslamian S (editor), Chapter 20, 433–453, CRC Press
- Veza P, Comoglio C, Rosso M, Viglione A (2010) Low flows regionalization in North-Western Italy. *Water Resour Manag* 24(14):4049–4074. <https://doi.org/10.1007/s11269-010-9647-3>
- Vogel RM, Kroll CN (1992) Regional geohydrologic-geomorphic relationships for the estimation of low-flow statistics. *Water Resour Res* 28(9):2451–2458. <https://doi.org/10.1029/92WR01007>
- World Meteorological Organization (WMO) (1974) *International glossary of hydrology*. World Meteorological Organization, Genève
- Yu PS, Yang TC, Liu CW (2002) A regional model of low flow for Southern Taiwan. *Hydrol Process* 16(10):2017–2034. <https://doi.org/10.1002/hyp.399>
- Zecharias YB, Brutsaert W (1988) Recession characteristics of groundwater outflow and base flow from mountainous watersheds. *Water Resour Res* 24(10):1651–1658. <https://doi.org/10.1029/WR024i010p01651>

## Affiliations

Konstantina Risva<sup>1</sup> · Dionysios Nikolopoulos<sup>2</sup> · Andreas Efstratiadis<sup>2</sup> · Ioannis Nalbantis<sup>1</sup>

✉ Ioannis Nalbantis  
nalbant@central.ntua.gr

<sup>1</sup> Department of Infrastructure and Rural Development, School of Rural and Surveying Engineering, National Technical University of Athens, Athens, Greece

<sup>2</sup> Department of Water Resources and Environmental Engineering, School of Civil Engineering, National Technical University of Athens, Athens, Greece